JOURNAL OF MATERIALS SCIENCE 18 (1983) 571–581

Transformation behaviour of the metastable phases in rapidly solidified Pd–Ge alloys

R. C. BUDHANI, T. G. GOEL, K. L. CHOPRA
Department of Physics, Indian Institute of Technology, Delhi, New Delhi-110 016, India

Rapid solidification from the melt by a melt-spinning technique is reported for Pd_xGe_{1-x} ($0.75 \leqslant x \leqslant 0.85$) alloys. The structure and transformation behaviour of the metastable phases so formed are investigated using X-ray diffraction, electron microscopy, differential thermal analysis and resistivity measurements. A glassy phase is observed in the alloys with Ge concentrations of 20% and 22.5%. This structure transforms to the equilibrium phases through a single-step process with an activation energy of 2.7 eV. In alloys with a lower Ge concentration, the as-quenched structure is a mixture of b c c ($a = 0.3077$ nm) and hexagonal ($a = 0.7460$ nm and $c = 1.2403$ nm) phases.

1. Introduction

Detailed studies [1] carried out in our laboratory on vapour-deposited Ge-alloy films have shown that Ge forms glasses with the 3d and 4d transition elements. On liquid quenching, however, Ge does not appear to form a glass with any of the 3d transition metals [2–6]. With the 4d and 5d series elements such as Pd, Pt and Au, liquid quenching at appreciably high cooling rates has been found to lead to metastable phases and also a glassy phase near the eutectic composition [2, 3]. The transformation behaviour of the metastable structures and maximum glass forming range for Pd–Ge alloys are not known, even in the light of a recent phase diagram [8]. A study of the crystallization behaviour of this system and its correlation with well-studied binary systems such as Fe–B [9], Pd–Si [10] and Au–Si [11] would help in establishing the role of the metalloid atomic diameter and the presence of a deep eutectic on the formation and stability of transition metal–metalloid (T–M) type glasses.

In this paper, we report our results on rapidly solidified Pd_xGe_{1-x} ($0.75 \leqslant x \leqslant 0.85$) alloys. The transformation behaviour of the metastable phases has been studied using X-ray diffraction, electron microscopy, electron diffraction, differential thermal analysis and resistivity measurements. The kinetics of amorphous to crystalline transformation has been established by monitoring changes in the electrical resistivity at various isothermal annealing temperatures.

2. Experimental procedure

Pd_xGe_{1-x} ($0.75 \leqslant x \leqslant 0.85$) alloys, in steps of $x = 0.025$, were prepared by electron-beam melting of the high-purity constituent metals in a water-cooled copper hearth. The alloy material was melted several times to ensure compositional homogeneity. About 4 g alloy was melt-spun in an argon atmosphere using a single roller technique [12]. The linear speed of the roller during preparation of the samples was $\sim 40\,m\,sec^{-1}$. The ribbons so formed were 1 to 1.5 mm wide amd 25 to 30 μm thick. The composition of the ribbons was checked using a scanning Auger microprobe. For thermal analysis, the ribbons were cut into small pieces, weighing about 5 mg, and placed in a Pt crucible of the high-sensitivity cell of a DTA (Stanton Redcroft 673-4 type) apparatus. Al_2O_3 powder was used as reference in an identical crucible. The transformation temperatures and heats of transformation were obtained by calibrating the instrument to the melting peaks of Sn and Pb. Structure of the as-quenched and annealed ribbons and microstructural changes during annealing were studied using X-ray diffractometry (Cu$K\alpha$, $\lambda = 0.154\,18$ nm) and transmission electron microscopy (AEI – EM 802 type). Samples for microscopy were

0022–2461/83/020571–11$03.82/0

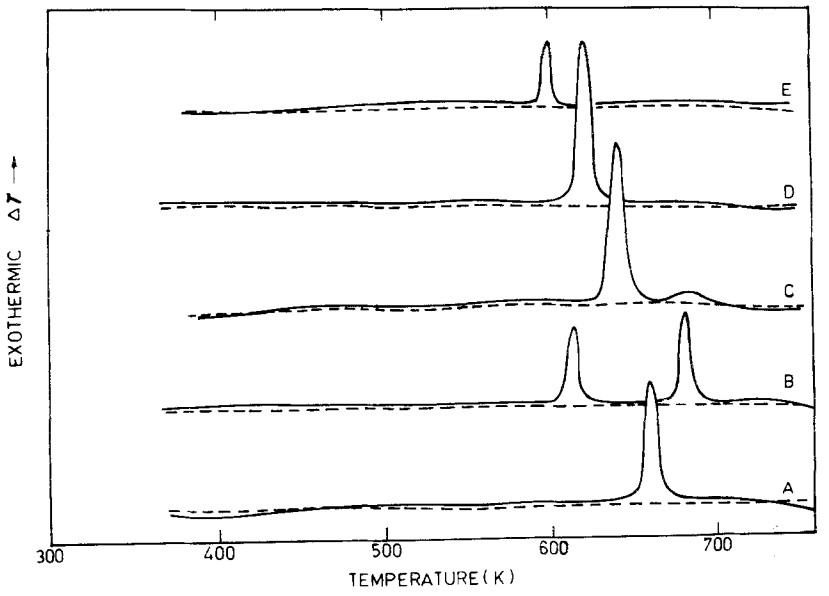

Figure 1 DTA thermograms of Pd_xGe_{1-x} ($0.75 \leqslant x \leqslant 0.85$) ribbons obtained by heating at 10 K min^{-1}.

thinned with a jet electro-polishing technique developed in the laboratory. The electrolyte used for polishing was a mixture of 70% acetic acid and 30% perchloric acid. The glass to crystalline transformation was also studied under isothermal and isochronal annealing conditions by monitoring the change in the electrical resistance of the sample by means of a standard four-probe technique.

3. Results

3.1. Thermal analysis

Fig. 1 shows the DTA thermograms of the five alloys, designated A, B, C, D, and E, with increasing Ge concentration, taken during the heating and cooling cycles. For alloys E and D, the themograms show a single exothermic peak at 600 and 625 K, respectively. For the C type ribbons, the main exothermic peak occurring at 642 K is followed by a broad hump which peaks at ~ 683 K. In the case of B type ribbons, a clear two-step exothermic effect, with two sharp peaks at 615 and 680 K, is observed. The A type ribbons show one exothermic peak at 660 K. The heats evolved during the transformations are listed in Table I.

3.2. Structural studies

X-ray diffraction studies revealed a glassy structure in the ribbons with 20% and 22.5% Ge concentration. Fig. 2 shows diffractograms of the $Pd_{80}Ge_{20}$ ribbons in the as-quenched and annealed states. The diffraction pattern of the as-quenched ribbons is characterized by two broad intensity distributions which peak at $2\theta = 40°$ and 72°. To study structural transformations corresponding to exothermic effects in the thermograms of these alloys, isothermal annealing was carried out at three different temperatures for 1 h each. As seen from Fig. 2, annealing 50 K below the crystallization temperature leads to a partially transformed glass. On annealing at the crystallization temperature, a complete transformation to the crystalline state takes place. Annealing 100 K above the transformation temperature does not bring any change in the structure except the

TABLE I Summary of the DTA results

Alloy	Ge (%)	T_1(K)	T_2(K)	$(\Delta H_c)T_1$ (cal mol^{-1})	$(\Delta H_c)T_2$ (cal mol^{-1})
A	15.0	660	–	608	–
B	17.5	615	680	320	497
C	20.0	642	683	687	62
D	22.5	625	–	663	–
E	25.0	600	–	123	–

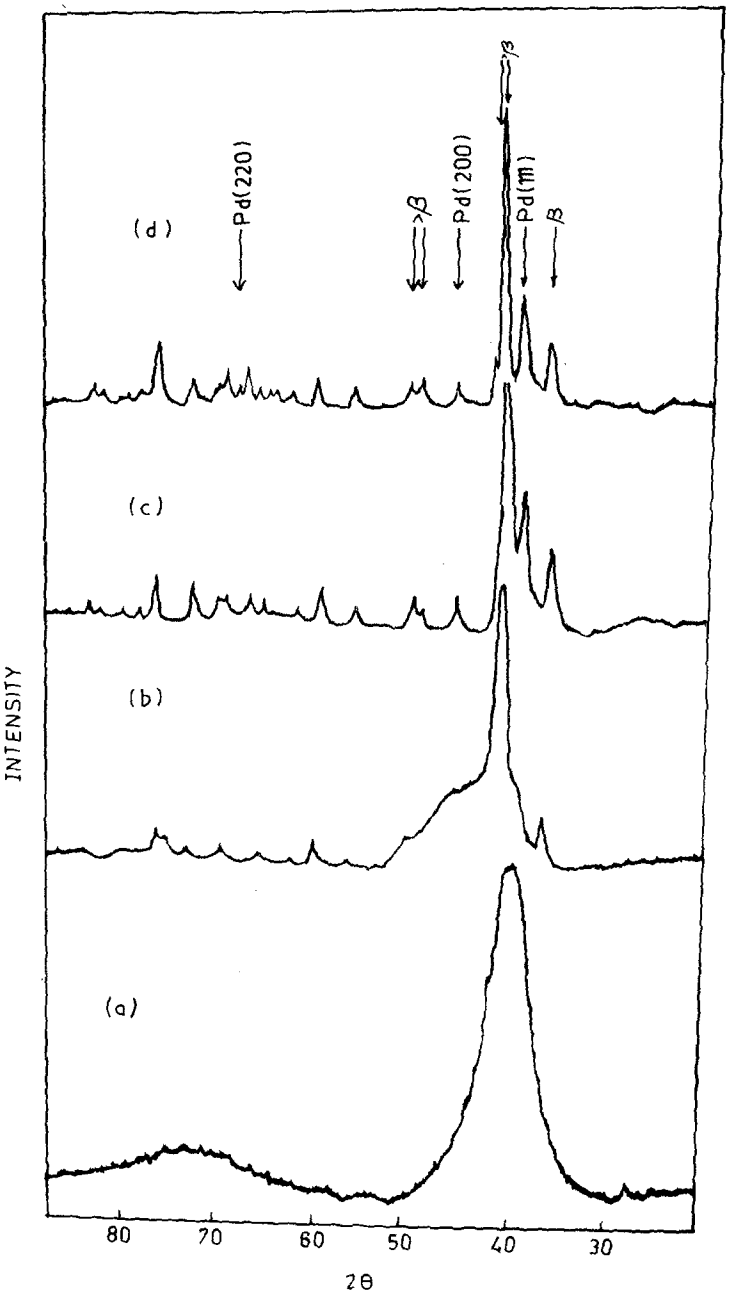

Figure 2 X-ray diffractograms of the $Pd_{80}Ge_{20}$ ribbons: (a) as-quenched, (b), (c) and (d) annealed at 50 K below T_c, at T_c, and 100 K above T_c, respectively, each for 1 h. Lines marked β (denoting $Pd_{25}Ge_9$) match the values reported by Nava *et al.*

sharpening of the lines, which presumably is due to the grain growth. Indexing of the lines which appear during three stages of annealing reveals that the glass transforms to a two-phase mixture consisting of α-Pd (fcc, $a = 0.39.16$ nm) and a germanide of palladium. Nava *et al.* [13] have studied the growth kinetics of various germanides at the palladium–germanium interface. A comparison of our X-ray data with the results of these workers shows that the germanide has the stoichiometry $Pd_{25}Ge_9$. Interplanar spacings for this phase are listed in Table II. It should be pointed out that the equilibrium phase diagram of this system, reported by Khalaff and Schubert [8] shows that the equilibrium phases at this composition are Pd_5Ge and Pd_3Ge. In our studies, however, the Pd_5Ge phase has not been detected.

Transmission electron micrographs and the corresponding electron diffraction patterns of the amorphous samples and the samples annealed at the crystallization temperature are shown in Fig. 3a and b. The diffraction vector corresponding to the halo in the electron diffraction pattern is the same as calculated from the X-ray diffrac-

TABLE II Interplanar spacings calculated from the X-ray diffraction pattern of $Pd_{80}Ge_{20}$ glass crystallized at 680 K for 1 h (Fig. 2d)

Interplanar spacings (nm)	$\frac{I}{I_{max}} \times 100$	Interplanar spacing (nm)	$\frac{I}{I_{max}} \times 100$
02.962	3	01.430	5
02.435	19	01.412	6
02.265 (α-Pd)	35	01.388	12
02.162	100	01.372 (α-Pd)	6
02.127	28	01.349	12
01.758 (α-Pd)	6	01.296	9
01.830	9	01.247	22
01.794	9	01.221	6
01.699	2	01.202	4
01.624	5	01.190	4
01.586	9		
01.481	4		
01.445	5		

tion data. The micrograph of the crystallized sample shows a two-phase mixture consisting of f c c-Pd and $Pd_{25}Ge_9$.

X-ray diffractograms of the $Pd_{82.5}Ge_{17.5}$ alloy, in the as-quenched and annealed states, are shown in Fig. 4. For the as-quenched alloy, the diffraction pattern consists of six lines. On annealing at 615 K for 15 min, the second line ($2\theta = 41° 6'$) of the diffractogram merges into the main peak ($2\theta = 41° 52'$) so that the diffraction pattern comprises of the five lines of the as-quenched alloy and some additional reflections. Annealing at the second exotherm (683 K) for 1 h, leads to a complete transformation to the f c c-Pd and $Pd_{25}Ge_9$. For a clear identification of the structures existing in the as-quenched and annealed

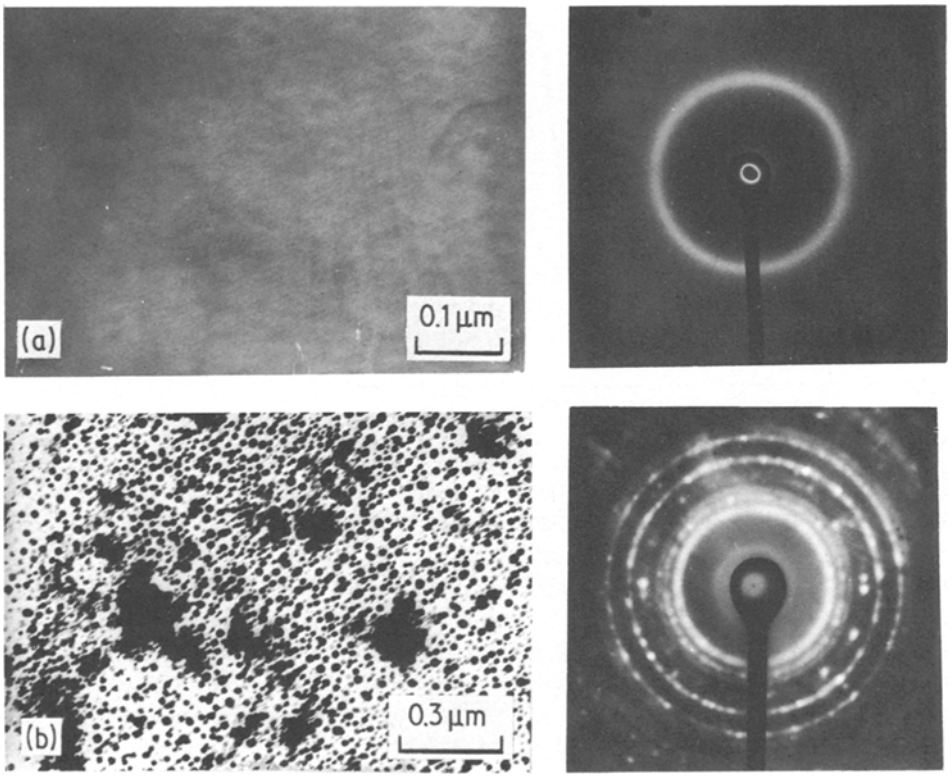

Figure 3 Selected-area electron diffraction pattern and corresponding electron micrographs of $Pd_{80}Ge_{20}$ ribbons, (a) as-quenched, and (b) annealed at the crystallization temperature.

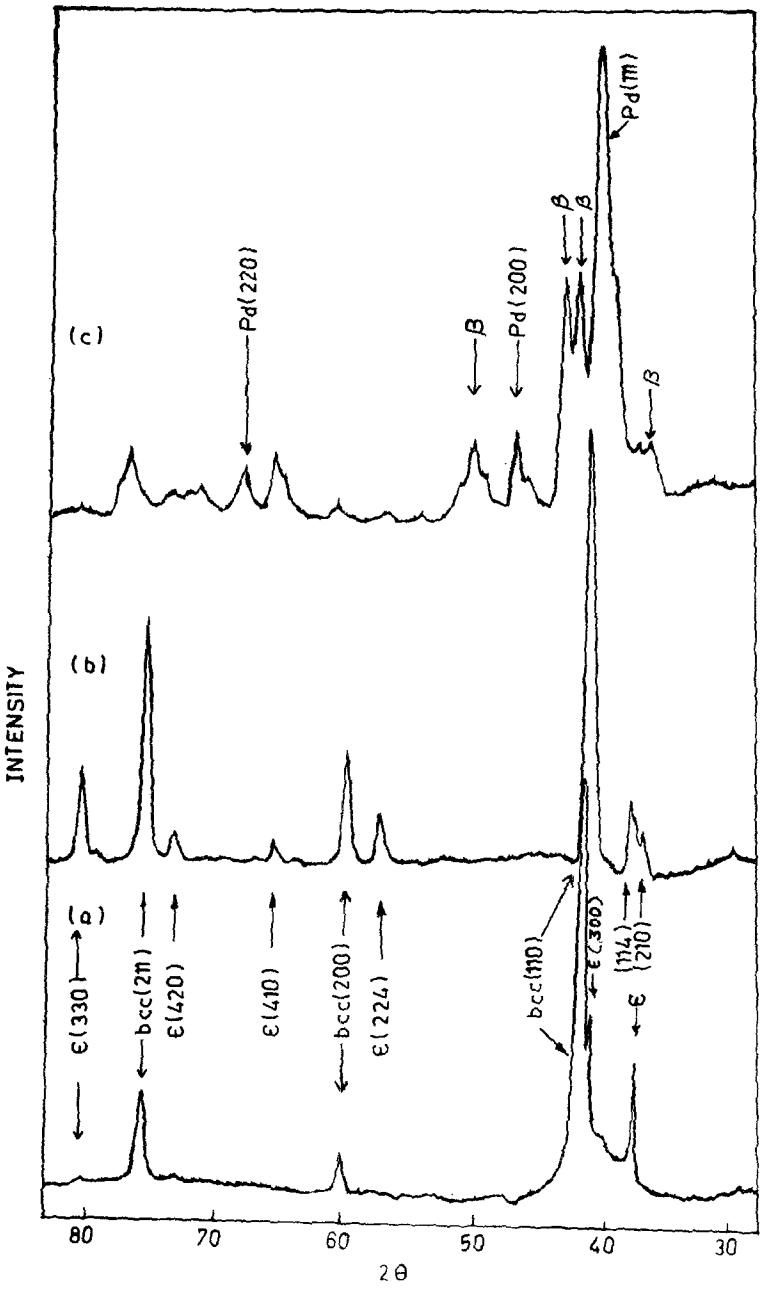

Figure 4 X-ray diffractograms of $Pd_{82.5}Ge_{17.5}$ ribbons: (a) as-quenched, (b) annealed at the first exotherm (615 K) for 15 min, and (c) annealed at the second exotherm (680 K). Lines marked ε denote the hexagonal phase.

samples, electron diffraction studies were carried out. Selected-area diffractions from the peripheral regions of the electrochemically etched holes in the as-quenched specimen are shown in Fig. 5a and b. The appearance of diffraction haloes (Fig. 5a) shows that the as-quenched structure consists of glass. The spots in the pattern correspond to a bcc ($a = 0.30.77$ nm) structure. Some regions of the sample also show a diffraction pattern (Fig. 5b) which appears to be a hexagonal structure grown perpendicular to the specimen plane.

The results of selected-area electron diffraction studies on the samples annealed at the first and second stages are shown in Fig. 6a and b, respectively. It can be seen that first-stage annealing leads to a two-phase mixture. The "d" values for these structures correspond to the bcc phase (Fig. 5a) and a phase which has been indexed tentatively on the basis of a hexagonal unit cell with $a = 0.7460$ nm and $c = 1.2403$ nm. Interplanar spacings of the bcc and hexagonal structures are listed in Table IIa and b. Second-stage anneal-

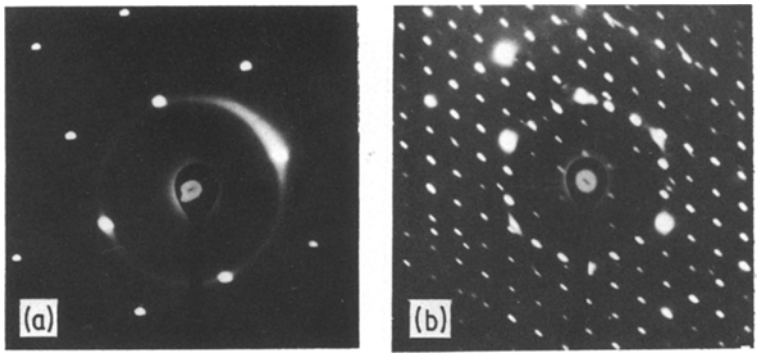

Figure 5 Selected-area electron diffraction patterns obtained from the as-quenched $Pd_{82.5}Ge_{17.5}$ ribbons: (a) amorphous plus bcc (b), preferential growth of a hexagonal phase.

ing leads to a complete transformation of the metastable bcc and hexagonal phases into the equilibrium alloys (Fig. 6b).

From a comparative study of the electron and X-ray diffraction data, it can be seen that the first two lines in the X-ray diffraction pattern (Fig. 4a) are the most intense reflections of the hexagonal structure which grows preferentially with the *c*-axis normal to the ribbon plane. The remaining four lines of the pattern correspond to the cubic structure. The overall transformation behaviour of the alloy is shown schematically in Fig. 7.

The exact stoichiometry of the bcc phase could not be obtained. However, from lattice parameter measurements, and taking into account the radius of palladium atom, it appears to be a metastable form of elemental Pd. A similar structure has also been reported by Duwez [7] in splat-quenched $Pd_{82}Ge_{18}$ alloys. However, the lattice parameter and transformation behaviour of this phase are not known.

X-ray analysis of the as-quenched $Pd_{85}Ge_{15}$ alloy revealed a structure which is the same as that observed after the first-stage annealing of

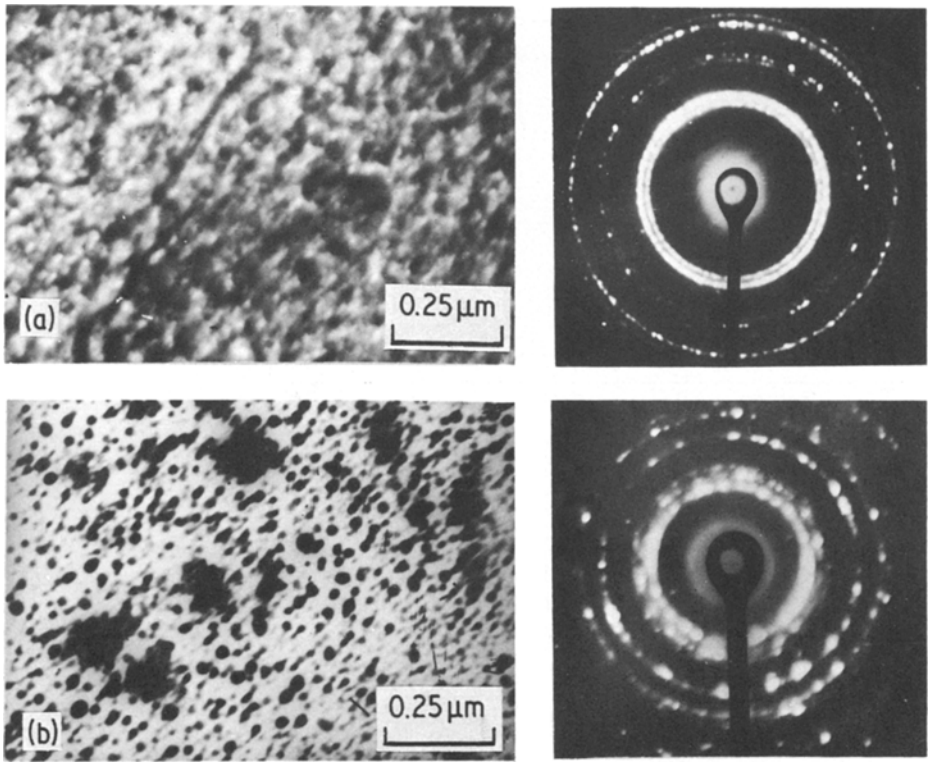

Figure 6 Selected-area electron diffraction and corresponding micrographs of the $Pd_{82.5}Ge_{17.5}$ ribbons, (a) annealed at the first exotherm (615 K) for 15 min, and (b) annealed at the second exotherm (680 K) for 1 h.

TABLE III X-ray and electron diffraction results for (a) the bcc phase and (b) the hexagonal phase observed in as-quenched $Pd_{82.5}Ge_{17.5}$ alloy

d (nm) (X-ray diff.)	Intensity	d (nm) (electron diff.)	Intensity	hkl	Lattice parameter (nm) (X-ray diff.)
(a)					
0.2162	100	0.217	s	(1 1 0)	
01.539	70	0.155	s	(2 0 0)	
0.1257	60	0.127	s	(2 1 1)	
		0.108	w	(2 2 0)	0.3077
		0.098	s	(3 1 0)	
		0.089	s	(2 2 2)	
		0.083	w	(3 2 1)	
		0.079	w	(4 0 0)	
(b)					
–	–	0.640	w	(1 0 0)	
–	–	0.365	ww	(1 1 0)	
–	–	0.320	w	(2 0 0)	
0.2412	8	0.242	s	(2 1 0)	$a = 0.7456$
0.2351	12	–		(1 1 4)	
0.2172(bcc)	100	0.216	vs	(3 0 0)	$c = 1.2403$
		0.184	vw	(2 2 0)	
0.1599	20	–	–	(2 2 4)	
0.1539(bcc)	20	–	–	–	
0.1419	5	0.142	s	(4 1 0)	
0.1031	4	–	–	–	
0.1287	6	0.127	w	(4 2 0)	
0.1254(bcc)	38				
0.1188	16	0.120	w	(3 3 0)	

$Pd_{82.5}Ge_{17.5}$. In the alloy with 25% germanium, the as-quenched structure was a mixture of the glass and the equilibrium crystalline phases. The exothermic effect in the thermogram of this alloy presumably marks the transformation of the glassy phase.

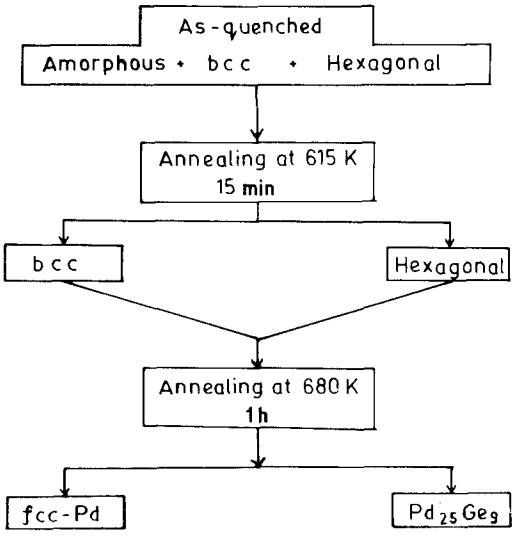

Figure 7 Flow chart, showing transformation sequence on annealing of melt-spun $Pd_{82.5}Ge_{17.5}$ specimens.

3.3. Kinetics of transformation of the glassy phase

The variation of the electrical resistance, R_T, normalized to the room temperature value, R_0, of the two alloys with 20% and 22.5% Ge is shown in Fig. 8. The heating rate during the measurements was 10° C min^{-1}. For the alloys with 20% Ge, the specific resistance (ρ) is high (~ 100 $\mu\Omega$cm) and increases with temperature with a small temperature coefficient $[(1/\rho)(dP/dT) = 1.87 \times 10^{-4}$ $K^{-1}]$. For ribbons with 22.5% Ge, the resistivity and its temperature coefficient are $\sim 126\,\mu\Omega$cm and 1.09×10^{-4} K^{-1}, respectively. In both cases, the resistivity increases slightly before crystallization and then drops sharply as crystallization proceeds. To study the kinetics of the amorphous to crystalline transformation, isothermal annealing of the as-quenched samples was performed at various annealing temperatures. Fig. 9 shows the variation of the normalized resistance of $Pd_{80}Ge_{20}$ ribbons as a function of

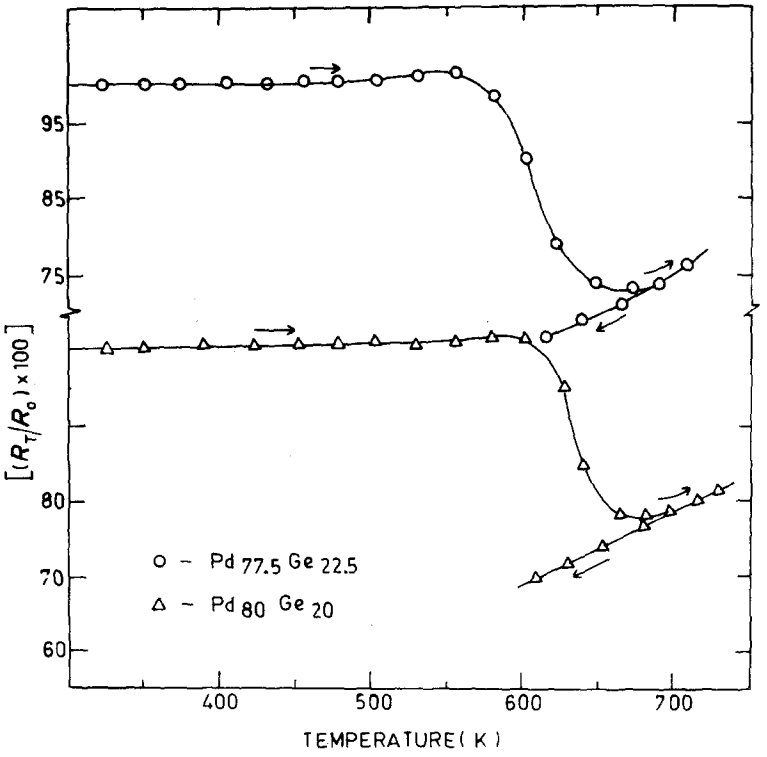

Figure 8 Variation of normalized resistance (R_T/R_0) with temperature for $Pd_{80}Ge_{20}$ and $Pd_{77.5}Ge_{22.5}$, continuously heated at 10° C min^{-1} through the temperature range 300 to 710 K.

annealing time for different annealing temperatures. Initially the resistance increases slightly for 5 min during which the furnace attains the isothermal annealing temperature. This value of resistance has been taken as R_{t0}. Once the temperature is reached, resistance falls gradually with time as the crystallization progresses. The time variation of the resistance may be used in understanding crystallization kinetics. The fraction of a material transformed in a time t, can be written as

$$\epsilon(t) = \frac{V_{cryst}(t)}{V_0}, \qquad (1)$$

where $V_{cryst}(t)$ is the volume of the material transformed in time t, and V_0 is the initial total volume of the non-crystalline material. Clearly, $\epsilon(t) = 0$ and 1 at $t = 0$ and $t = \infty$, respectively.

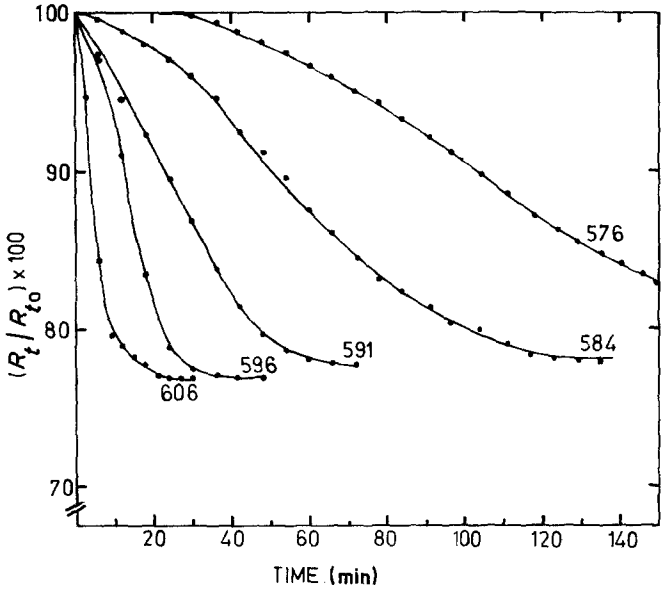

Figure 9 Variation of the normalized resistance of $Pd_{80}Ge_{20}$ glass with time at different annealing temperatures.

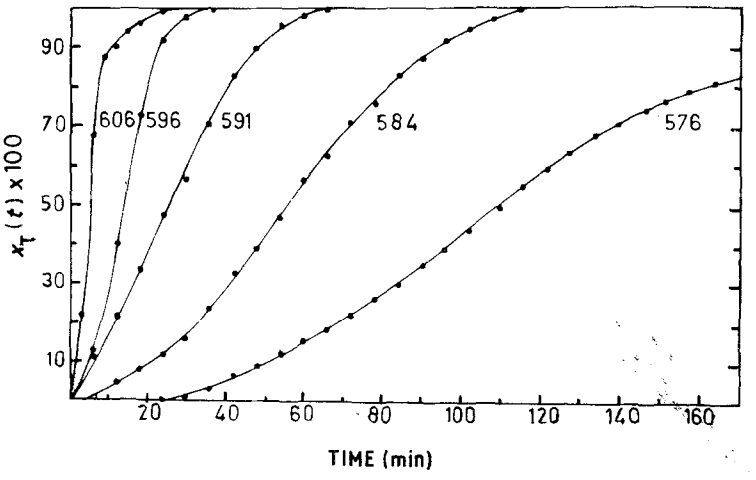

Figure 10 Volume fraction of glassy $Pd_{80}Ge_{20}$ alloy transformed as a function of time for various annealing temperatures.

A similar quantity can de defined in terms of the resistivity as

$$X_T(t) = \frac{(R_{t0} - R_t)}{(R_{t0} - R_M)}, \quad (2)$$

where R_{t0}, R_t and R_M are the resistances of the material initially, at time t and at the end of the transformation, respectively. If the isothermal annealing temperature is close to the crystallization temperature, $X_T(t)$ approaches unity in finite time. For a nucleation and growth type transformation process, $\epsilon(t)$ follows the Johnson–Mehl–Avrami rate equation [13]:

$$\epsilon(t) = 1 - \exp(-Kt^n), \quad (3)$$

where K is the kinetic constant and the exponent, n, is a characteristic of the mode of the transformation. Since in a metallic system, the resistivity closely tracks the microstructural changes, a one to one correspondence can be assumed between $\epsilon(t)$ and $X_T(t)$. On this basis Equation 3 can be rewritten as

$$X_T(t) = 1 - \exp(-Kt^n). \quad (4)$$

Fig. 10 shows the resulting time dependence of the volume fraction, $X_T(t)$, of the material crystallized at different isothermal annealing temperatures. The temperature dependence of the crystallization rate can be obtained by defining a time constant τ, at which $X_T(\tau) = 1/2$. The time constant follows the Arrhenius form [14]:

$$\tau = \tau_0 \exp \frac{\Delta E}{k_B T}, \quad (5)$$

where k_B is the Boltzman constant and ΔE the activation energy for the transformation. ΔE can be evaluated by plotting ln τ against $1/T$. The variation of ln τ with $1/T$ is shown in Fig. 11 and the value of ΔE so obtained is 2.7 eV. A similar calculation for $Pd_{77.5}Ge_{22.5}$ yields ΔE of the same magnitude.

To calculate the Avrami index n, Equation 5 at time t and τ can be combined to arrive at

$$-\frac{\ln [1 - X(t)]}{\ln 2} = \left(\frac{t}{\tau}\right)^n. \quad (6)$$

The exponent n can be calculated by fitting the plot of $-\ln [1 - X(t)]/\ln 2$ against (t/τ) with a curve derived from an equation of the form $y \propto x^n$. As shown in Fig. 12, for $Pd_{80}Ge_{20}$ glass,

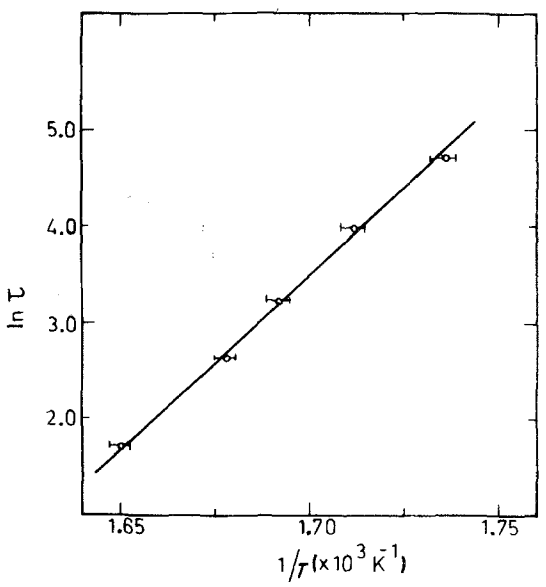

Figure 11 Determination of the activation energy for crystallization of $Pd_{80}Ge_{20}$ alloy from a plot of ln τ $1/T$ plot.

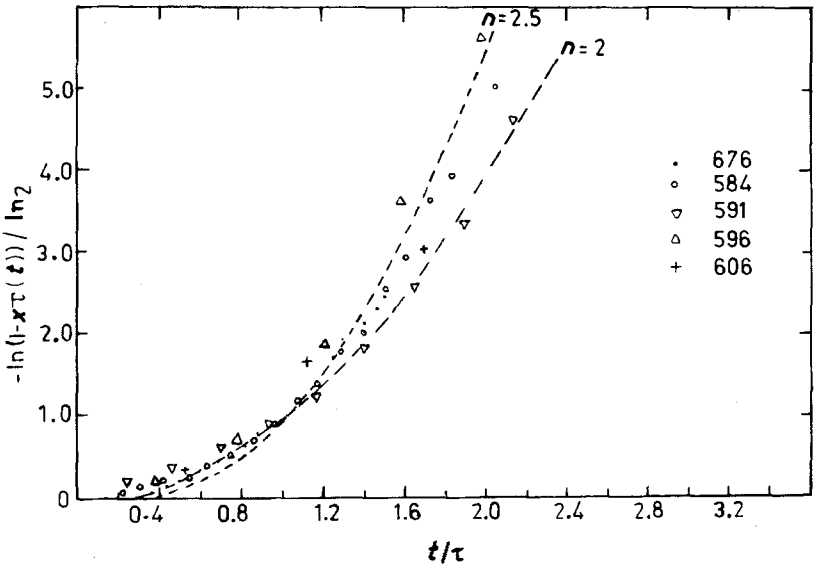

Figure 12 A plot of $-\ln [1 - X_T(t)]/\ln 2$ against t/τ for $Pd_{80}Ge_{20}$ alloy to obtain the Avrami index for crystallization.

the data agree for $y \propto x^2$ and $y \propto x^{2.5}$, leading thereby to $n = 2$ to 2.5.

4. Discussion

A varying degree of metastability can be obtained by rapid quenching of liquid metals and alloys [2, 3]. The extreme limit of such metastable structures correspond to freezing of the topologically random structure of the liquid. The formation and stability of the glassy structure is, however, decided by three factors:(i) the cooling rate and hence the rate of nucleation of a crystalline phase during the solidification process: (ii) the activation barrier for atomic movements to reach an equilibrium state; and (iii) the free energy difference between the glassy and crystalline structures. A comparison with the glass-forming ability of binary systems such as Fe–B [16] and Pd–Si [17] shows that the glass-forming range for the Pd–Ge system is narrow. For the alloy with a Ge concentration of 17.5%, the cooling rate is not enough to freeze-in the glassy structure. However, it is not sufficiently small to allow the equilibrium structure to nucleate. This intermediate situation apparently leads to some short-range adjustment of atoms and, thus, the formation of less metastable b c c and hexagonal phases.

The crystallization temperature (T_c) which is a measure of the relative thermal stability of different compositions, is maximum for the eutectic alloy ($Pd_{80}Ge_{20}$). This observation is similar to the behaviour of other transition metal–metalloid glasses. The highest T_c of the eutectic glasses has been attributed to the maximum filling of the voids by metalloid in a Bernal type [18, 19] structure of the metal atoms. However, the Goldschmidt radii of Pd and Ge are the same (0.137 nm). Such a filling, if necessary, would require the Ge to be present in the ionic form ($2r = 0.088$ nm). Our photoemission [20] and electron transport measurements [21], however, do not show the Ge in tetravalent ionic state (Ge^{4+}). Alternatively, the behaviour of T_c can be understood in terms of the maxima destabilization of the eutectic alloy [22].

Modes of the transformation of the non-crystalline phase to stable crystalline phase/phases are decided by the composition, atomic mobility and the relative stability of the final products [9]. The two-phase structure in the samples annealed at 50 K below T_c along with some non-crystalline phase, shows that the transformation is of eutectic decomposition type. Since no change in the structure was observed on annealing at 100 K above T_c, the broad hump in the thermogram of $Pd_{80}Ge_{20}$ alloy can be attributed to the completion of the transformation or some form of recrystallization as revealed by diffraction peak sharpening. This conclusion, based on X-ray data, is speculative. A more extensive TEM study would yield clearer information.

The activation energy calculated on the basis

of the Johnson–Mehl–Avrami rate equation is comparable with the activation energy for self-diffusion in crystalline palladium (2.6 eV above 1050 K) [23]. Activation energy for the diffusion of Ge in 4d transition element lattices is much smaller. For example, it is only 1.5 eV in Ag above 670 K. From these values, it appears that inter-diffusion of the components initiates the transformation process. The exact mechanism of the diffusion process in metallic glasses in general is, however, not well established [24].

Detailed work of Scott ([9] p. 198) on nickel- and iron-based metallic glasses, gives a value for the Avrami index, n, which varies between 3 and 4. The smaller value observed in our case is, however, not surprising in view of the fact that n being 3 and 4 indicates a continuous nucleation process. If nucleation takes place at the beginning of the transformation, the process is primarily growth-controlled with a characteristic index varying from 2 to 3. We feel that, for $Pd_{80}Ge_{20}$ glass, the nucleation occurs rapidly at the beginning of the transformation. Negligibly small incubation times observed for the crystallization process (Fig. 8) support this argument.

In conclusion, the glassy alloys of Pd–Ge transform to a two-phase mixture consisting of f c c-Pd and $Pd_{25}Ge_9$ on isothermal and isochronal annealing. The activation energy for the amorphous to crystalline transformation is 2.7 eV. The Avrami index $n = 2$ to 2.5, as calculated from the isothermal annealing behaviour of the resistivity, suggests that the transformation is a growth-dominated process. As-quenched alloys with Ge concentrations 17.5% and 15% are a complex mixture of a b c c ($a = 0.3077$ nm) and a hexagonal phase ($a = 0.746$ nm, $c = 1.2403$ nm) which on annealing transform to the equilibrium crystalline phases.

Acknowledgements

The authors are grateful to Mr V. D. Arora and Mr V. K. Dhar for valuable assistance in electron microscopy and X-ray diffraction studies, respectively.

References

1. H. S. RANDHAWA, P. NATH, L. K. MALHOTRA and K. L. CHOPRA, *Solid State Commun.* **20** (1976) 73.
2. H. S. RANDHAWA, L. K. MALHOTRA and K. L. CHOPRA, *J. Non-Cryst. Solids* **29** (1978) 311.
3. B. C. GIESSEN, in "Development in the Structural Chemistry of the Alloy Phases", edited by B. C. Giessen (Plenum Press, New York, 1969) p. 227.
4. S. TAKAYAMA, *J. Mater. Sci.* **11** (1976) 164.
5. H. JONES, *Rep. Prog. Phys.* **36** (1973) 1425.
6. C. SURYANARAYANA "Rapidly Quenched Metals – a Bibliography" (Plenum, New York, 1980).
7. P. DUWEZ, *Trans. Amer. Soc. Metals* **60** (1967) 607.
8. K. KHALAFF and K. SCHUBERT, *Z. Metallkde* **65** (1974) 379.
9. U. HAROLD and U. KOSTER, in Proceedings of the "Third International Conference on Rapidly Solidified Metals" Vol. I, edited by B. Cantor (The Metal Society, London, 1978) p. 281.
10. T. MASUMOTO and R. MADDIN, *Acta Metall.* **19** (1971) 725.
11. C. H. BENNETT, D. E. POLK and D. TURNBULL, *ibid.* **19** (1971) 1295.
12. R. C. BUDHANI, T. C. GOEL and K. L. CHOPRA, *Bull. Mat. Sci. (India)* in press.
13. F. NAVA, G. MAJNI, G. OTTAVIANI and E. GALLI, *Thin Solid Films* **77** (1981) 319.
14. J. W. CHRISTIAN, "Theory of Transformation in Metals and Alloys" (Pergamon, Oxford 1975).
15. C. P. CHOU and D. TURNBULL, *J. Non-Cryst. Solids* **19** (1975) 725.
16. P. E. LUBORSKY and H. H. LEIBERMANN, *Appl. Phys. Letters* **33** (1978) 233.
17. B. G. LEWIS and H. A. DAVIES, *Mater. Sci. Eng.* **23** (1976) 179.
18. J. D. BERNAL, *Nature* **185** (1960) 68.
19. D. E. POLK, *Acta Metall.* **20** (1972) 485.
20. R. C. BUSHANI, S. RAJAGOPALAN, A. BANERJEE, T. C. GOEL and K. L. CHOPRA, *Thin Solid Films* **89** (1982) 73.
21. R. C. BUDHANI, T. C. GOEL and K. L. CHOPRA, *J. Phys. F.* in press.
22. H. S. CHEN and B. K. PARK, *Acta Metall.* **21** (1973) 395.
23. C. J. SMITHELLS, "Metal Reference Book" (Butterworths, London, 1967).
24. R. W. CAHN, *Contemp. Phys.* **21** (1980) 43.

Received 24 May
and accepted 16 July 1982